Acta Geophysica (2023) 71:2989–3005
https://doi.org/10.1007/s11600-023-01121-5

RESEARCH ARTICLE - ATMOSPHERIC & SPACE SCIENCES

Assessment of reanalysis datasets against radiosonde observation over the Eastern Mediterranean region

Rokaya Mohamed Hassan[1] · Zeinab Salah[1] · Theodore Karacostas[2] · Mohamed Magdy Abdel-Wahab[3]

Received: 6 December 2022 / Accepted: 17 May 2023 / Published online: 5 June 2023

Abstract

Four meteorological components (geopotential height *Z*, air temperature *T*, dew point temperature Td, and relative humidity RH) collected from ERA-5 and ERA-Interim were compared with the observations of nine radiosonde stations with different climatic changes, at different isobaric levels (850, 700, 500, and 200 hPa) during the period 2000–2017, in order to assess the accuracy of the aforementioned reanalysis datasets. The results showed that both reanalysis datasets have a strong correlation with the observed variables, except with dew point temperature and relative humidity in the upper troposphere. The mean values of geopotential height and temperature from both grid dataset are generally consistent with the radiosonde values, whereas considerable bias in the mean Td and RH exists and increases upwards. The study clearly proved that the reanalysis datasets can be used to compensate for the lack of radiosonde observation. Furthermore, air temperature (during 1959–2021) showed an increasing trend from the surface to the lower troposphere, while the temperature decreased in the upper troposphere and lower stratosphere. Finally in this study, the impact of the North Atlantic Oscillation Index (NAOI) on the air temperature was also examined, and a negative relationship was found between NAOI and temperature at the levels: surface, 850, 700, and 500 hPa, while a positive relationship was found, only in winter, at 200 hPa. At the level of 100 hPa, the correlation is positive for both seasons.

Keywords ERA-5 · ERA-Interim · Radiosonde · Temperature · NAOI · Mediterranean area

Introduction

The Eastern Mediterranean region is characterized by frequent thunderstorms, during the winter seasons. Some are severe. The preconditions of the formation of thunderstorms are conditional instability of the atmosphere, a moist layer of sufficient depth in the lower or mid-troposphere, and a source of lift to initiate the convection (Johns and Doswell 1992). These conditions could be estimated using upper air meteorological variables. The upper air variables were obtained from three different methods: radiosonde observations, satellite data, and the reanalysis datasets. The advantage of the radiosonde data is that it has the longest historical time series with high vertical resolution. The lower numbers of stations in oceanic Polar Regions and discontinuities in historical times are disadvantages of the radiosonde. Even though the satellite data offer better coverage and horizontal resolution than radiosonde observations, they have lower vertical resolution and shorter time series. Reanalysis data can satisfy both requirements in terms of coverage and length of time series (Guo et al. 2016). The reanalysis data could be the solution to the biggest trigger meteorologist faces in forecasting thunderstorms, due to their rather small spatial and temporal extension (Orlanski 1975); even though their temporal and spatial distribution are small, they have catastrophic effects. Although the Eastern Mediterranean region is spacious, it contains a few radiosonde stations. Figure 1 shows the distribution of radiosonde stations in four countries Greece, Turkey, Cyprus, and Egypt according to the observing stations—weather reports—of World Meteorological Organization (WMO, 2012). There are only

Edited by Prof. Ioannis Pytharoulis (ASSOCIATE EDITOR) / Prof. Ramón Zúñiga (CO-EDITOR-IN-CHIEF).

✉ Rokaya Mohamed Hassan
rok.hassan@gmail.com; rokaya.hassan@ema.gov.eg

[1] Egyptian Meteorological Authority, Cairo, Egypt

[2] Department of Meteorology and Climatology, Aristotle University of Thessaloniki, Thessaloniki, Greece

[3] Faculty of Science Department of Astronomy, Space Science and Meteorology, Cairo University, Giza, Egypt

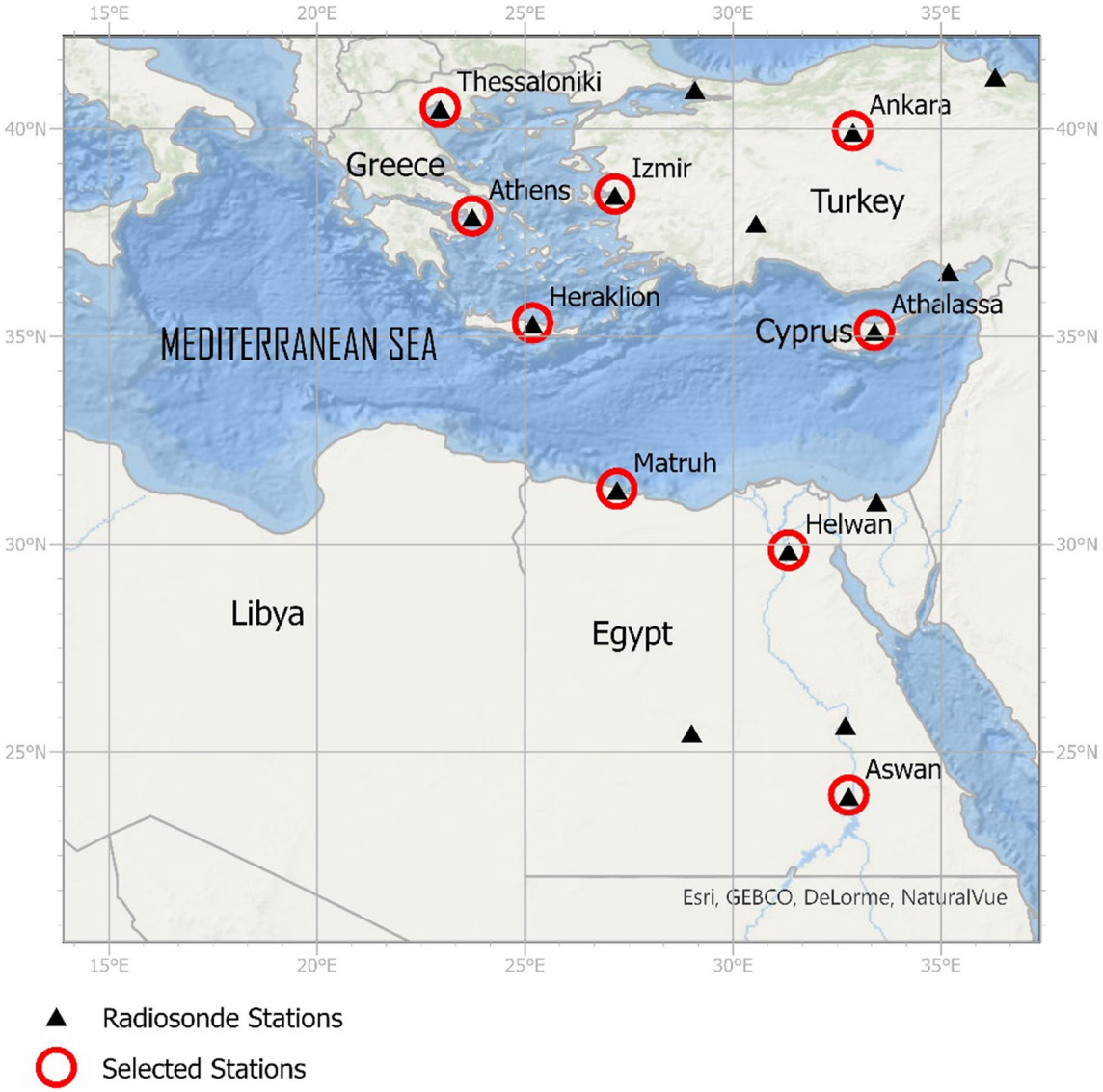

Fig. 1 Spatial distribution of radiosonde stations of Greece, Turkey, Cyprus, and Egypt according to the WMO (weather reporting volume A, 2012). The highlighted red circles are the selected stations in the study

16 radiosonde stations with a very low spatial distribution. They are insufficient for forecasting mesoscale severe weather phenomena such as thunderstorms. More radiosonde stations should be covered within the Mediterranean region, specifically in the Arabian Peninsula (Al-Hemoud et al. 2022).

Tan (2019) evaluated the radiosonde observation of the precipitable water with NCEP-NCAR for all radiosonde stations of Turkey using two methods of extracting the reanalysis data: the nearest grid point to the radiosonde locations and the bilinear interpolation method. She concluded that the bilinear interpolation method was much better to evaluate precipitable water, than the nearest grid point to the radiosonde locations. It was only applicable for the inland station and not reliable for coastal and mountainous regions, i.e., NCEP-NCAR cannot capture extreme values of precipitable water (Stickler et al. 2015) comparing the upper air data with reanalysis (20CR, ERA-20C) for the tropical and South Atlantic, and they found a good agreement between historical data and reanalysis. Bao and Zhang (2013) found consistency between sounding observation and four reanalysis data for temperature and wind, but there were differences with mean relative humidity. Fu et al. (2016) compared 22 climate variables at the surface and upper air using NCEP-NCAR and ERA-Interim datasets. Their results showed that the performance of ERA-Interim is better than NCEP-NCAR. Mooney et al. (2011) apply the comparison of three reanalysis datasets on surface temperature over Ireland on

land stations and marine buoys using four co-location techniques over the 1989–2001 period. They found the three reanalyses to be significantly warmer in winter than the observations but colder than the observation temperature of marine buoys located around the Irish coast.

The vertical temperature structure of the atmosphere is a primary indicator of climate change (Marshall 2002). According to IPCC (2013), the troposphere has warmed, and the stratosphere has cooled since the late twentieth century. This is consistent with Philandras et al. (2017) results about the climatology of upper air temperature over the Mediterranean region during the period 1965–2015. Elbessa et al. (2021) stated that the air temperature in the Southeastern Levantine Basin has a warming trend during the period 1989–2018. Tonbol et al. (2018) also get a warming trend of surface temperature for the same area of study. The highest mean annual temperature was recorded at the year 2010.

The North Atlantic Oscillation Index (NAOI) is the difference of atmospheric pressures at mean sea level between measured values in the Azores at 38°N and Iceland at 65°N (Hurrell and Deser 2009). NAO has two phases: positive NAO + and negative NAO−. Different phases of the NAO affect the temperature and precipitation. The influence of NAO on extreme temperature is higher than on extreme precipitation in the Arab region (Donat et al. 2014). Hasanean, (2004) and Shaltout et al. (2013) studied how both phases of NAO affect air temperature, precipitation, and mean sea-level pressure. They have significantly correlated with the NAO index in winter. When winters are cold, NAO index has positive values, and in warmer winters the NAO index is negative. High (low) winter precipitation occurred with positive (negative) NAO index values.

The current study was carried out to verify different meteorological variables at different pressure levels from two reanalysis datasets: ERA-Interim and ERA-5 against the sounding data at nine stations representing different climatic characteristics in the Eastern Mediterranean region. Moreover, it was aimed to find an alternative source for upper air data by using the reanalysis data to compensate for the lack of in situ observation at the study area. The ERA-5 data was available from 1959 to 2021 and was used to study the surface and upper air temperature climatology over the Eastern Mediterranean region. Finaly find the impact of the North Atlantic Oscillation (NAO) index n the surface and upper air temperature during summer and winter.

Data and methodology

Observed upper air data

The observed daily upper air data used in this study were obtained from the University of Wyoming site (http://www.weather.uwyo.edu/) of nine synoptic weather stations with different climatic characteristics, for the period 2000–2017. According to the Köppen classification, the stations were chosen to represent the different climatological conditions. The locations of the stations and their latitudes, longitudes, height from mean sea level, and climate type are given in Table 1.

ERA-Interim data

ERA-Interim (Dee et al. 2011), which was produced by ECMWF, uses 4D-variational analysis on a spectral grid with triangular truncation of 255 waves (corresponding to approximately 80 km) and a hybrid vertical coordinate system with 60 levels. This reanalysis covers the period from 1979 to 2019. The ERA-Interim data used in this study were obtained from the ECMWF data server on a fixed grid of 0.125 degrees.

ERA5 data

ERA5 has been produced by ECMWF replacing the ERA-Interim reanalysis. ERA5 provides hourly estimates of a large number of atmospheric, land, and oceanic climate variables. The data cover the Earth on a 30 km grid and resolve the atmosphere using 137 levels from the surface up to a height of 80 km. ERA5 combines vast amounts of

Table 1 The stations' lat, lon, height from the MSL, and climate type

Station	Lat	Lon	Height (m)	Climate	Köppen-Geiger
Ankara	39.95 N	32.88E	891	Cold semiarid	Bsk
Aswan	23.96 N	32.78 E	194	Hot desert climates (Semitropical)	Bwh
Athalassa	35.15 N	33.4 E	161	Hot-summer Mediterranean climate	Csa
Athens	37.9 N	23.73 E	15	Dry-summer subtropical climate	Csa
Helwan	29.86 N	31.33 E	141	Hot desert climates (Urban)	Bwh
Heraklion	35.33 N	25.18 E	39	Hot-summer Mediterranean climate	Csa
Izmir	38.43 N	27.16 E	29	Dry-summer subtropical climate	Csa
Matruh	31.33 N	27.21 E	28	Hot desert climates (Coastal)	Bwh
Thessaloniki	40.51 N	22.96 E	4	Humid subtropical climate	Cfa

historical observations into global estimates, compared to ERA-Interim, using 4D-Var data assimilation in CY41R2 of ECMWF's Integrated Forecast System (IFS). This reanalysis covers the period from 1959 to the present. The ERA5 data used in this study were obtained from the ECMWF data server on a fixed grid of 0.25 degrees (Hersbach and Dee, 2016).

NAOI

Data of the NAOI—monthly data—were obtained from https://climatedataguide.ucar.edu/climate-data/hurrell-north-atlantic-oscillation-nao-index-station-based for the period 1959–2021 and using ERA-5 data of air temperature of the same period.

Methodology

Upper air variables data were obtained from the Department of Atmospheric Science, the University of Wyoming, with two reanalysis datasets ERA-interim and ERA-5. The variables are geopotential height *Z*, temperature *T*, dew point temperature Td, and relative humidity RH, at four pressure levels 850, 700, 500, and 200 hPa, using the daily values at 00 UTC of the period 2000–2017, except at station Athalassa, where the available radiosonde data are at 12 UTC.

The following statistical values were calculated: mean bias (MB), root-mean-square error (RMSE), Pearson correlation coefficient (*r*), and the standard deviation ratio (*S*). These values obtain the difference, how much error, correlation, and similarity of the dispersion between the observed and reanalysis data, respectively. The mean bias is an index for evaluating the accuracy of reanalysis data.

The smaller mean bias in the simulation conveys more effective results. The RMSE represents the variation degree in the mean bias. When calculating the mean bias, the observed data were subtracted from the reanalysis datasets. Thus, positive (negative) results of mean bias indicate overestimated (underestimated) values of the reanalysis.

The Pearson correlation was applied between the North Atlantic Oscillation Index (NAOI) and the surface and upper air temperature anomalies at selected barometric levels to examine the impact of atmospheric circulation on the surface and upper air temperature for the period 1959–2021. The statistical significance of the correlation coefficients was calculated.

Results and discussion

Vertical profile

Figures 2, 3 and 4 show the vertical profiles of the statistical parameters: *r,* MB*,* and RMSE, respectively, of radiosonde variables (*Z*, *T*, Td, and RH) with ERA-Interim and ERA-5, during the period 2000–2017 at the nine examined stations. The correlation is very strong regarding *Z* at all levels and increases with altitude (Fig. 2a). However, the MB and RMSE of *Z* indicate less concordance. The values of the MB are increased with altitude as it is indicated in Fig. 3a, with some exceptions, where it decreased with the altitude for ERA-Interim, at stations such as Ankara, Athalassa, Heraklion, Izmir, and Thessaloniki. Athens is the only station where the ERA-Interim and ERA-5 overestimated the *Z* at all levels. The rest of the stations depict underestimation with respect to both reanalysis data, except Aswan at 850 hPa in the case of ERA-5, and Athalassa at 200 hPa in the case of ERA-Interim. RMSE also increases with altitude, as it is demonstrated in Fig. 4a. The values of RMSE corresponding to ERA-5 are relatively higher in the upper troposphere compared to ERA-Interim values, except for Athens.

The comparative analysis of T obtained a very strong correlation at all levels, indicated in Fig. 2b. Aswan has the lowest r, but is still strong with a value of $r > 0.9$. The correlation results are consistent with Gleixner et al. (2020), and they found that temperature correlation with ERA-5 is slightly higher than that with ERA-Interim applying temperature correlation in Africa. They recommended using ERA-5, because it has a high agreement with observations. Figure 2b shows the correlation of temperature with ERA-5 is higher than with ERA-Interim; except in Aswan the correlation of temperature with ERA-Interim is slightly higher than with ERA-5, and at all levels it is obvious at 850 hPa, see (Fig. 2b). This distinction may refer to the climatology of Aswan, which differs from those of other stations. Values of MB are small and decrease with altitude (Fig. 3b). The RMSE values, shown in Fig. 4b, decrease from 850 to 500 hPa and increase again to 200 hPa. The increase in the temperature RMSE at 200 hPa is probably due to the occurrence of the jet stream around that level (Woyciechowska and Bąkowski 2006). Td and RH have similar vertical profile patterns for the statistical parameters; r is very strong at low levels, and the highest correlation is found at the level 700 hPa. Then, it decreases with altitude the lowest r which was at Izmir 0.28 and 0.36 for Td and RH, respectively, in Fig. 2c, d. The MB was positive at 850 hPa at Athens, Heraklion, Izmir, and Matruh for both Td and RH and then

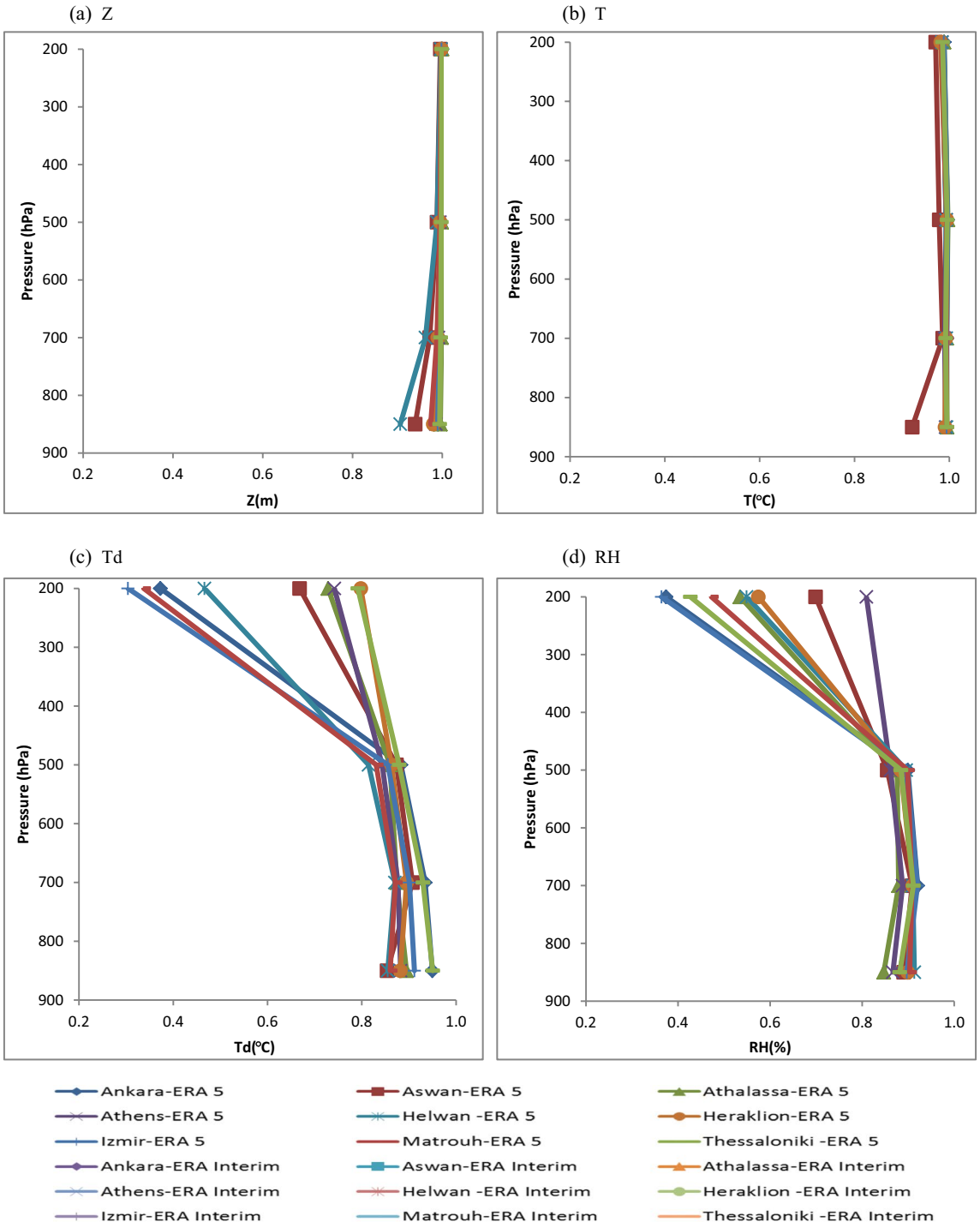

Fig. 2 Vertical profiles of Pearson correlation coefficient r between radiosonde observed variables **a** Z, **b** T, **c** Td, and **d** RH and the ERA-Interim and ERA-5, at the 9 examined stations

became negative. This means the reanalysis datasets underestimate the observation at the lower troposphere and overestimated at the upper levels in Fig. 3c, d. This may be due to the locality and climate of these stations; all are coastal stations. The rest of the stations were overestimated. Both

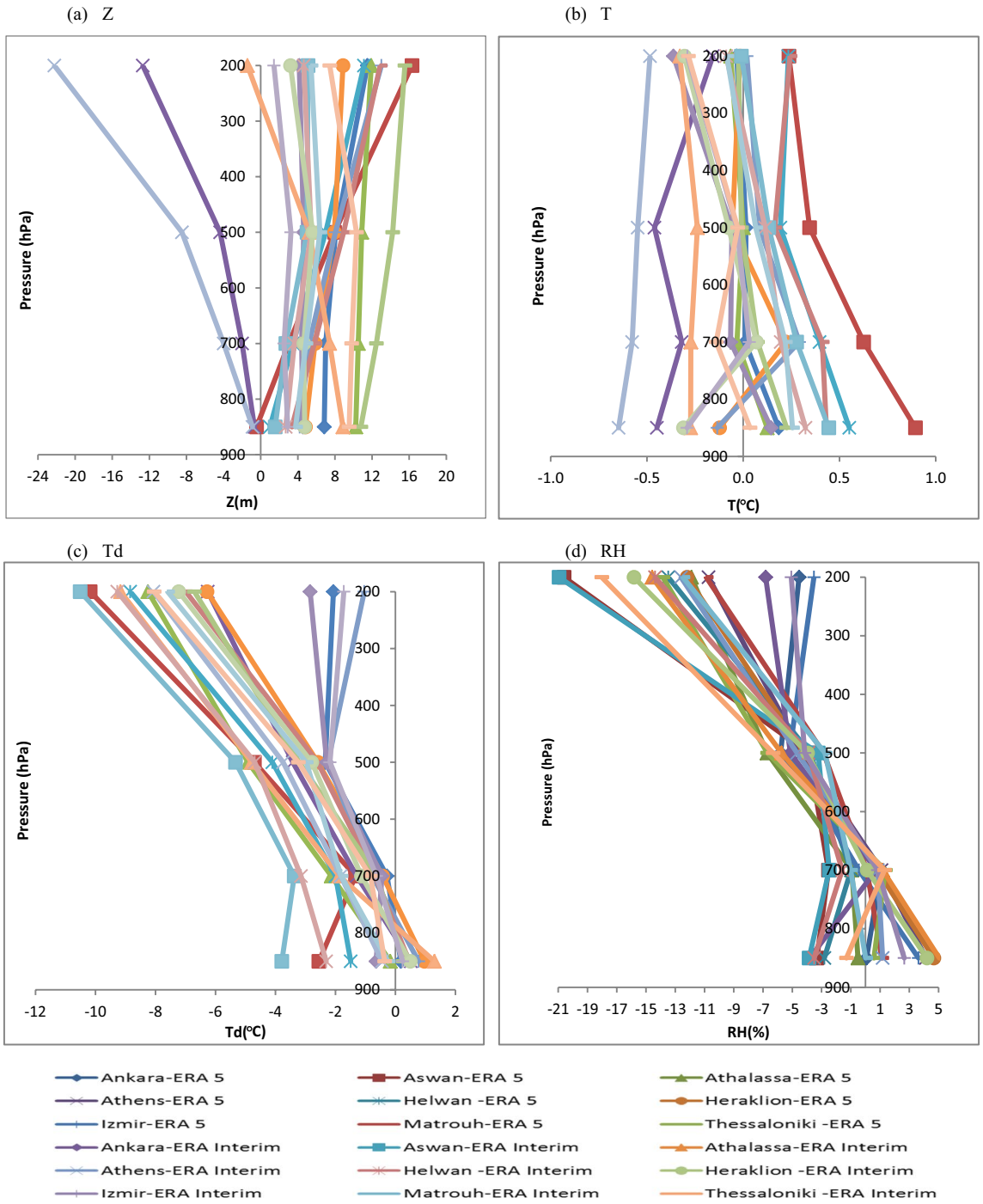

Fig. 3 Vertical profiles of mean bias (MB) between radiosonde observed variables **a** Z, **b** T, **c** Td, and **d** and the ERA-Interim and ERA-5, at the 9 examined stations

MB and RMSE values increase with altitude as indicated in Fig. 4c, d. The largest bias and error were counted at 200 hPa in Aswan 12 °C, 27%, respectively; its climate is semitropical. The quality of the moisture in the upper air may be highly uncertain, due to the large RMSE between the reanalysis data and sounding observation (Bao and Zhang 2013; Dong et al. 2017).

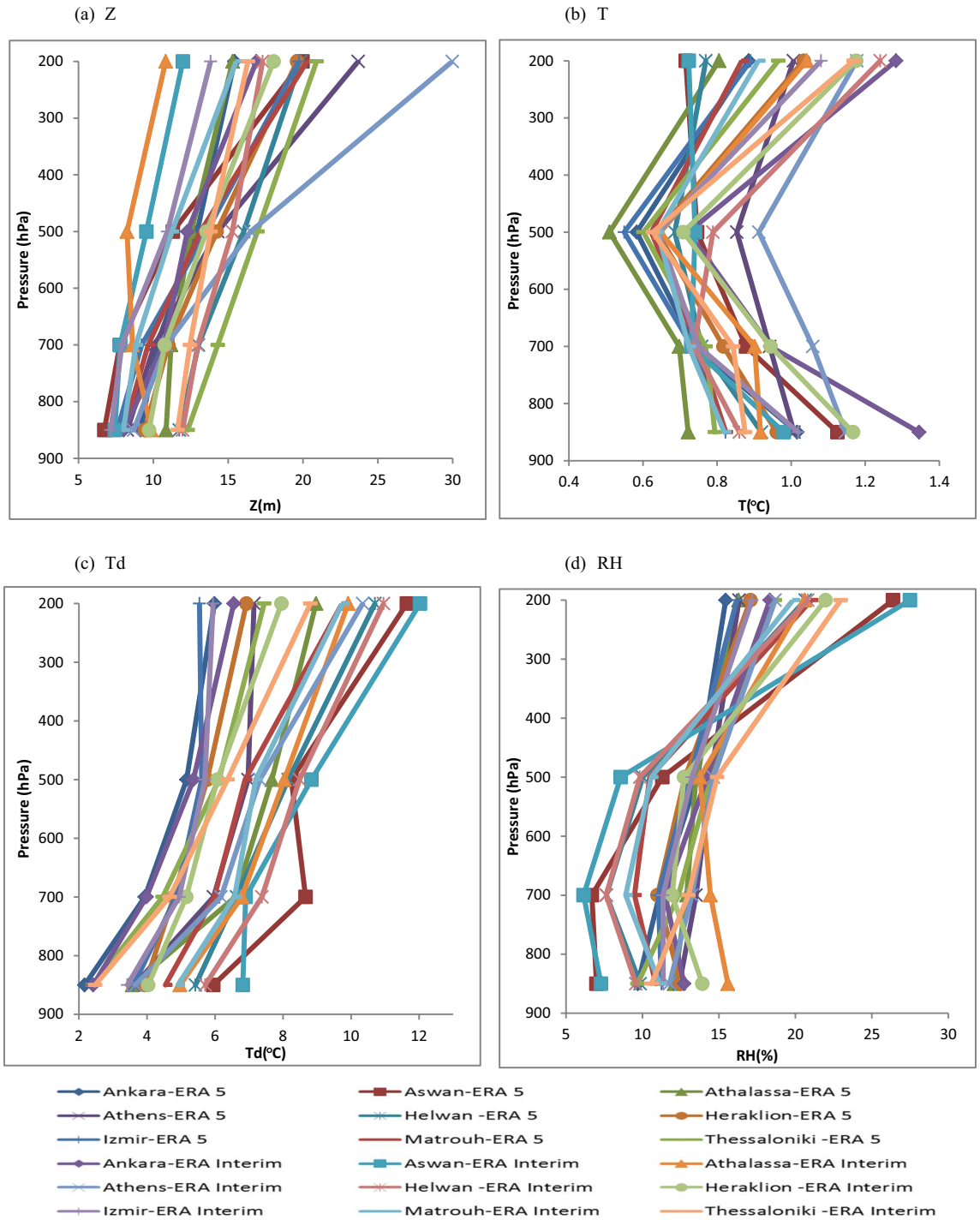

Fig. 4 Vertical profiles of root-mean-square error (RMSE) between radiosonde observed variables **a** Z, **b** T, **c** Td, and **d** RH and the ERA-Interim and ERA-5, at the 9 examined stations

Taylor diagram

Taylor diagram (Taylor 2001) is used to demonstrate the similarity of the variability and dispersion as well, by comparing the correlation and standard deviations of the daily upper air variables (*T*, *Z*, Td, and RH), as they are illustrated in Figs. 5, 6, 7 and 8, during the period 2000–2017, at the different examined levels. The correlation is statistically significant at 95% confidences level. For the temperature, the correlations of the observed

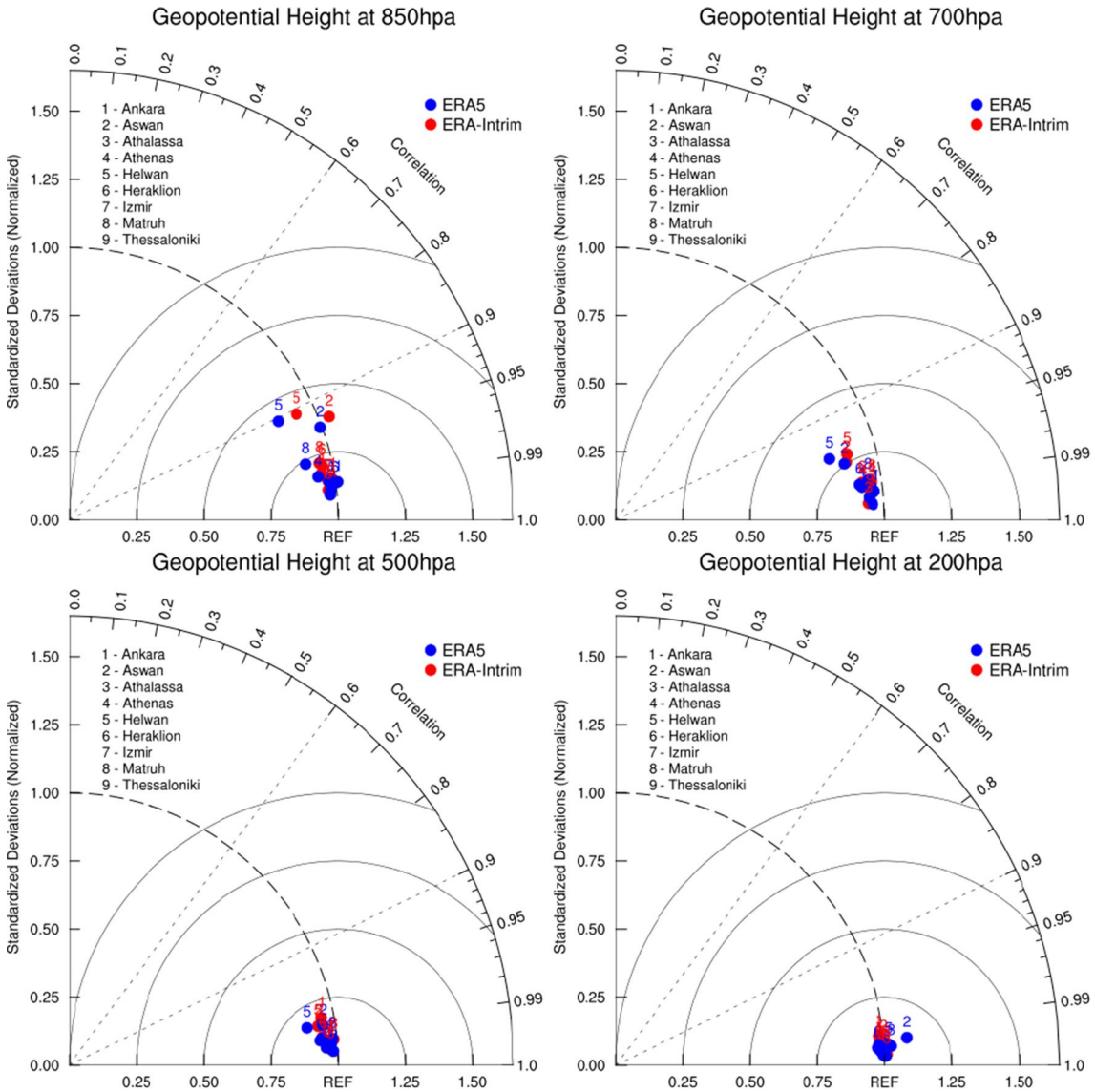

Fig. 5 Taylor diagram for daily geopotential height Z of ERA-5 (blue) and ERA-Interim (red) versus observed radiosonde observations for the nine stations. For the isobaric level 850, 700, 500, and 200 hPa during the period 2000–2017

data with ERA-Interim and ERA-5 are very strong and always higher than 0.9 for all levels, whereas the ratio of the reanalyzed data to the observed standard deviation is much close to 1. In addition, the geopotential height has a strong correlation, and the ratio is close to 1. The correlation of the dew point temperature (Fig. 7) is less than 0.9, with a ratio lower than 1, and decreases with altitude till it becomes less than 0.5 at 200 hPa. Relative humidity has a correlation between the observed and reanalysis data around 0.9 at the lower level, which decreases at the level of 200 hPa with a ratio close to 1 at low levels and increases rapidly with altitude. In 200 hPa for relative humidity, the decrease in correlation and increase in ratio between reanalysis and radiosonde causes all stations to be out of scale, except for Matruh station, which appears on the border with correlation less than 0.5 and ratio about 1.7 as shown in Fig. 8. As a result, the reanalysis data cannot represent relative humidity at 200 hPa.

Slope of scatter plot

The linear relationship between the reanalysis datasets and observation was explained by studying the scatter plot between them. Slope values must be around 1.0. According to (Mooney et al. 2011), the perfect agreement between the observation and the reanalysis datasets occurs with a slope equal to 1.0 and an intercept value of 0.0, in order

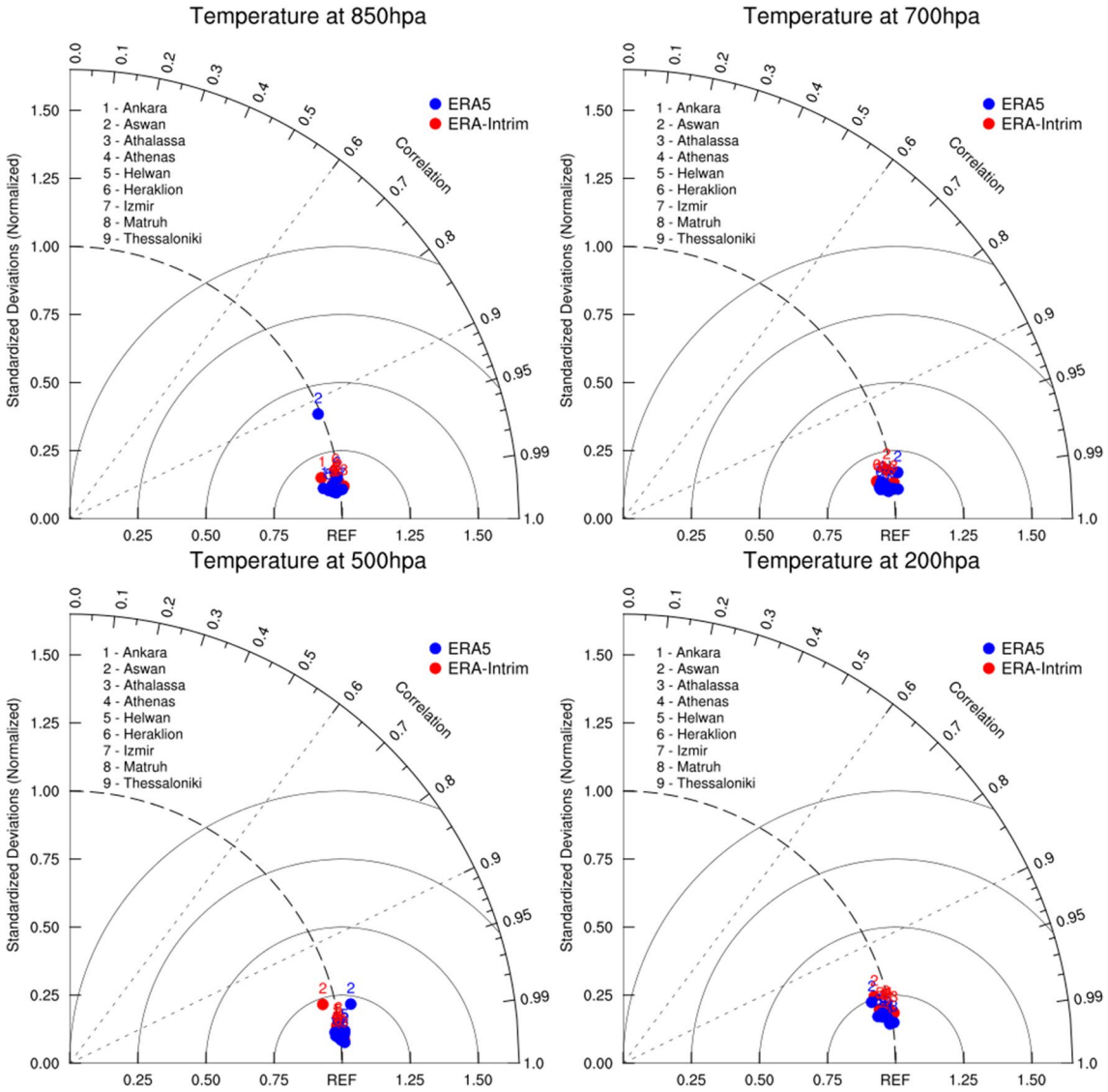

Fig. 6 Same as Fig. 5 but for the temperature T

to get a good agreement between surface temperature and reanalysis datasets over Ireland. Here, the slopes were calculated between the reanalysis datasets and observation for the nine stations at different levels as they are presented in Tables 2, 3, 4 and 5 for the variables *Z*, *T*, Td, and RH, respectively. There is a good agreement between the reanalysis datasets and observation for *Z*, and *T*; nine stations show a slope greater than 0.84 in the case of *Z*, and greater than 0.93 for *T*. The value of the slope decreases upwards till it reached its lowest value at 200 hPa for Td, as indicated in Izmir and Matruh stations. Slope values greater than 1.0 appear only with RH at 200 hPa for both datasets (Table 5).

According to (Baatz et al. 2021), the difference between ERA-5 and ERA-Interim is slightly small, so they can be used to compensate for the lack of radiosonde observation data considered the reanalysis data an alternative solution to observational data, which has continuous temporal and spatial coverage.

Climatology of surface and upper air temperature

From the previous findings, the air temperature of ERA-5 has a good agreement at all levels with observed radiosonde. This section uses the ERA-5 data of the air temperature of the surface, 850, 500, 200, and 100 hPa to study some climatological characteristics of surface and upper air temperature, by applying the Mann–Kendall trend analysis for winter (DJF) and summer (JJA) months through the period 1959–2021. Figure 9 shows the spatial distribution

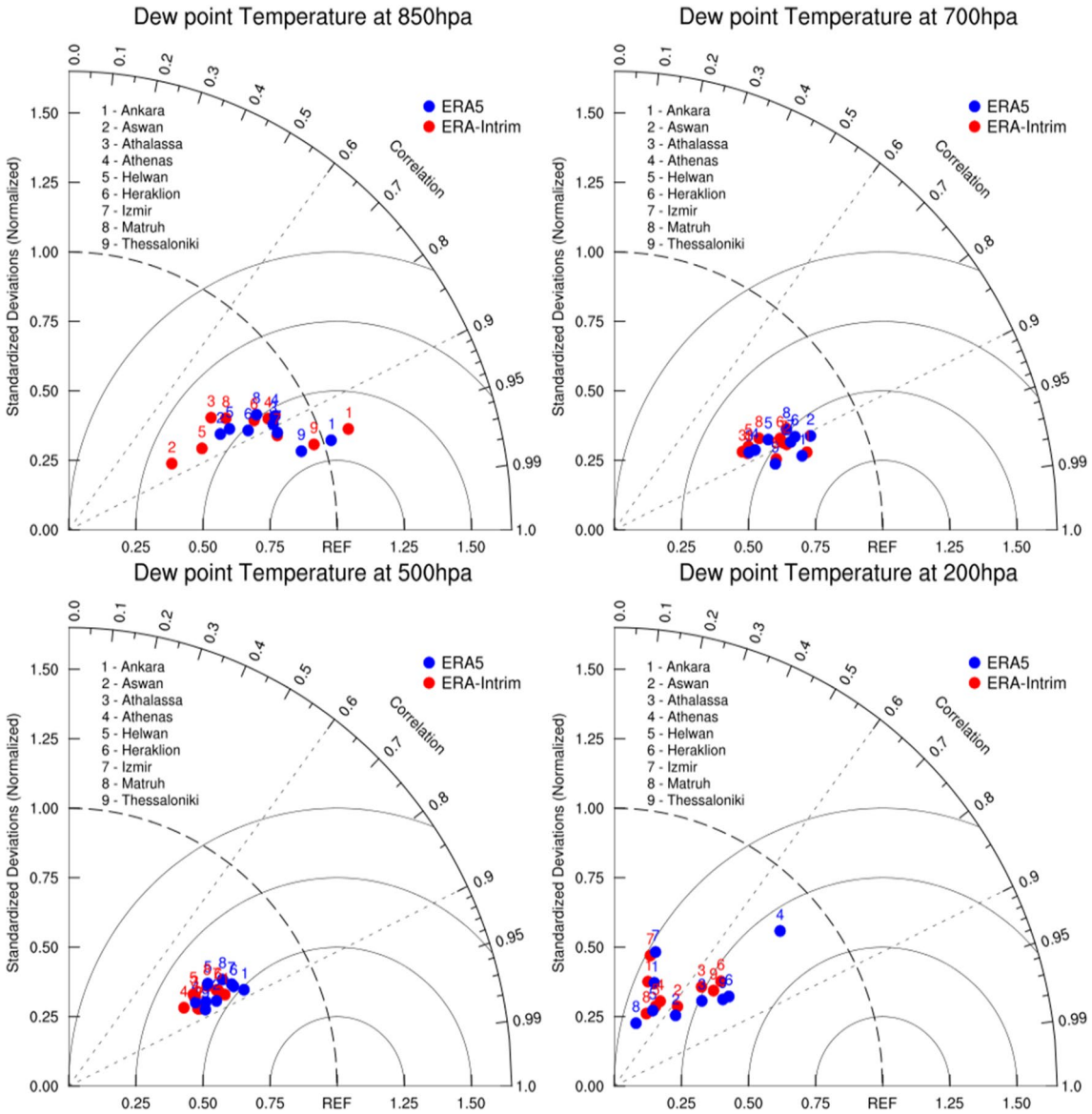

Fig. 7 Same as Fig. 5 but for the dew point temperature Td

Table 2 Slope of scatter plot between radiosonde and reanalyses for *Z*

Z slope	ERA-5				ERA-Interim			
Station	850	700	500	200	850	700	500	200
Ankara	0.99	0.98	0.98	1.00	0.98	0.97	0.98	1.00
Aswan	0.94	0.92	0.97	1.00	0.95	0.91	0.96	1.00
Athalassa	0.98	0.98	0.99	1.00	0.98	0.97	0.98	1.00
Athens	0.96	0.95	0.97	0.99	0.96	0.95	0.97	0.99
Helwan	0.85	0.90	0.95	0.98	0.88	0.91	0.96	0.99
Heraklion	0.95	0.95	0.96	0.98	0.96	0.95	0.97	0.99
Izmir	0.98	0.98	0.99	1.00	0.98	0.97	0.98	1.00
Matruh	0.94	0.96	0.98	1.00	0.95	0.97	0.99	1.00
Thessaloniki	0.98	0.97	0.98	0.99	0.98	0.97	0.98	0.99

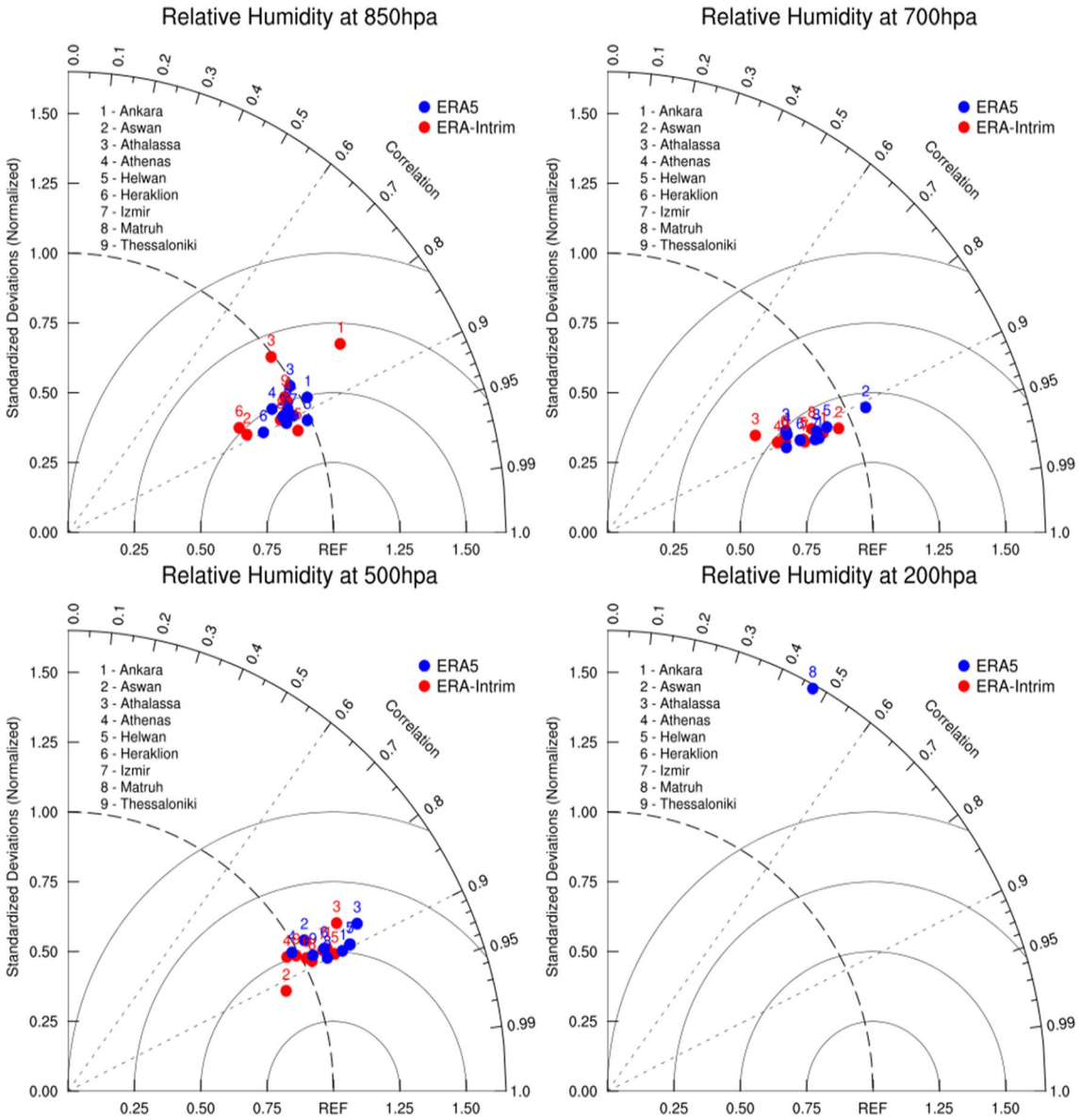

Fig. 8 Same as Fig. 5 but for the relative humidity RH

Table 3 Slope of scatter plot between radiosonde and reanalyses for *T*

T slope	ERA-5				ERA-Interim			
Station	850	700	500	200	850	700	500	200
Ankara	0.96	0.98	1.00	0.98	0.95	0.97	0.99	0.98
Aswan	0.91	0.98	0.98	0.95	0.99	0.98	0.95	0.94
Athalassa	0.99	1.00	1.00	0.99	1.00	0.99	1.00	0.99
Athens	0.98	0.97	0.98	0.97	0.98	0.96	0.98	0.97
Helwan	0.98	0.97	0.99	0.96	0.98	0.98	0.99	0.94
Heraklion	0.99	0.97	0.99	0.97	0.98	0.96	0.99	0.97
Izmir	1.00	0.98	1.00	0.98	0.99	0.98	1.00	0.98
Matruh	0.99	0.98	0.99	0.97	0.99	0.99	1.00	0.97
Thessaloniki	0.98	0.98	0.99	0.98	0.98	0.97	0.99	0.97

Table 4 Slope of scatter plot between radiosonde and reanalyses for Td

Td slope	ERA-5				ERA-Interim			
Station	850	700	500	200	850	700	500	200
Ankara	0.96	0.81	0.76	0.24	0.99	0.82	0.71	0.20
Aswan	0.69	0.81	0.69	0.39	0.57	0.76	0.65	0.39
Athalassa	0.83	0.66	0.66	0.49	0.65	0.64	0.62	0.47
Athens	0.82	0.68	0.63	0.68	0.81	0.66	0.60	0.29
Helwan	0.72	0.71	0.65	0.26	0.65	0.65	0.61	0.27
Heraklion	0.77	0.78	0.73	0.58	0.77	0.74	0.69	0.54
Izmir	0.84	0.77	0.72	0.22	0.84	0.75	0.68	0.19
Matruh	0.78	0.75	0.69	0.17	0.69	0.68	0.65	0.22
Thessaloniki	0.91	0.75	0.67	0.57	0.93	0.75	0.64	0.52

Table 5 Slope of scatter plot between radiosonde and reanalyses for RH

RH slope	ERA-5				ERA-Interim			
Station	850	700	500	200	850	700	500	200
Ankara	0.89	0.86	0.96	0.53	0.93	0.86	0.93	0.65
Aswan	0.85	0.94	0.87	1.40	0.77	0.89	0.87	1.43
Athalassa	0.84	0.77	0.98	1.03	0.77	0.69	0.93	1.21
Athens	0.82	0.77	0.85	1.76	0.85	0.76	0.84	1.77
Helwan	0.91	0.87	0.98	0.89	0.89	0.82	0.95	1.30
Heraklion	0.81	0.81	0.92	1.07	0.75	0.77	0.89	1.22
Izmir	0.87	0.85	0.98	0.51	0.85	0.83	0.92	0.56
Matruh	0.86	0.85	0.94	0.60	0.85	0.83	0.91	1.09
Thessaloniki	0.85	0.78	0.90	0.71	0.84	0.78	0.86	0.75

of the air temperature trend at all levels and the values of the trend (in ℃/Year) for the nine examined stations in Table 6. Almost all stations depict a significant trend (confidence level at 95%) for all levels, except in Matruh at the surface and the lower troposphere. The temperature trend of the Eastern Mediterranean indicates the effect of climate change by increasing the air temperature from the surface all the way to the isobaric level of 200 hPa. Then, the trend switched to negative and decreased the temperature at the level of 100 hPa. Temperature trend results in warming at the surface and lower troposphere, while cooling at the upper troposphere and lower stratosphere, which are consistent with many studies concerning the climatology of temperature (IPCC 2013; Philandras et al. 2017; Elbessa et al. 2021).

Surface and upper air temperature with NAOI

Although the teleconnection NAO is not the dominant circulation pattern in the Mediterranean region, according to (Philandras et al. 2015) it strongly influences its climate, particularly in wintertime.

Winter

The Pearson correlation between the NAOI and air temperature during winter months (DJF) for the period 1959–2021 was negative on the surface over Egypt, and the Eastern Mediterranean, while it was positive from the western parts of Turkey. The correlation at 850 hPa is similar to the surface, as shown in the left column of Fig. 10. At 500 hPa, it is also similar to the lower altitude, while the correlation

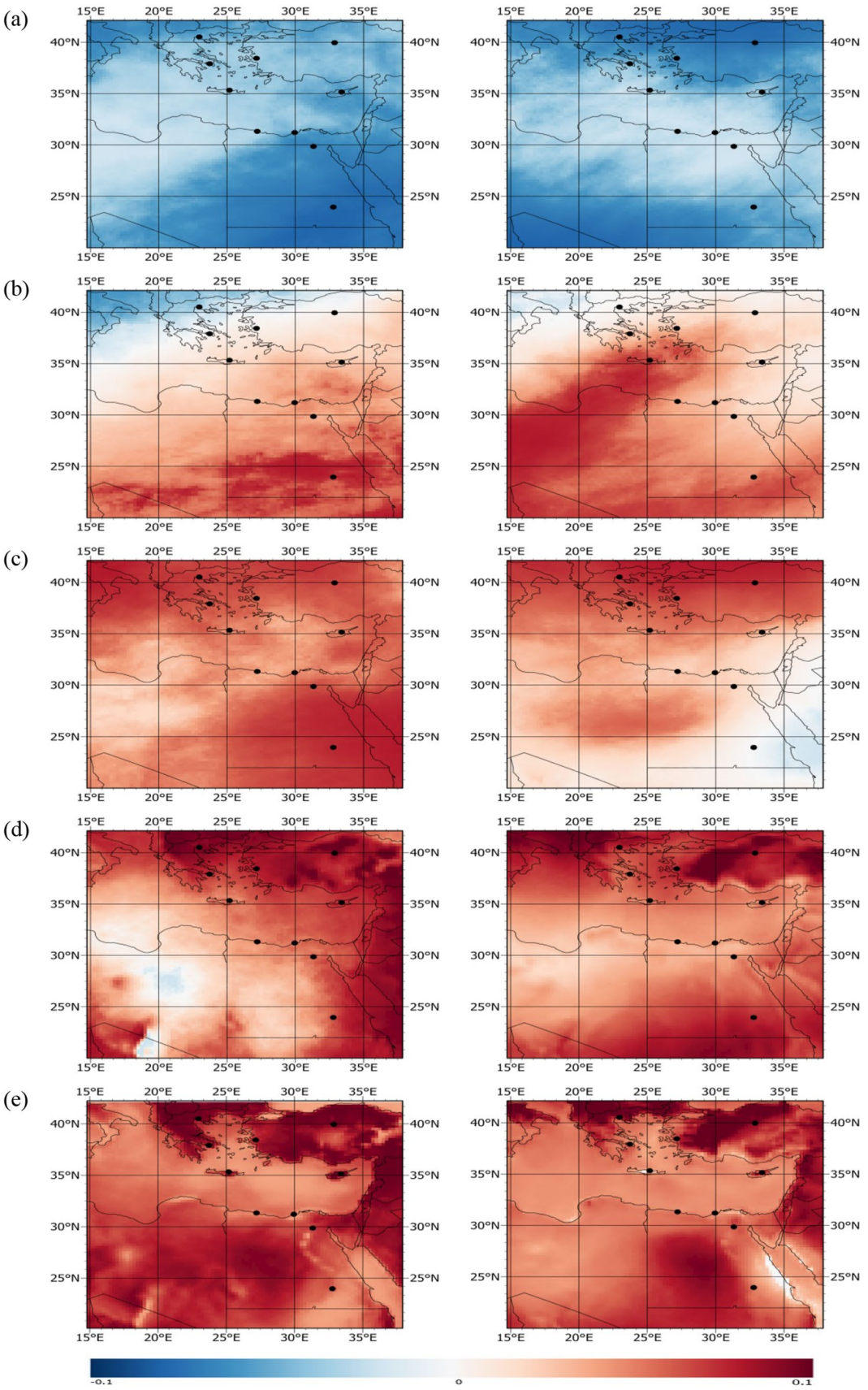

Fig. 9 Surface and upper air temperature trends (ºC/year) 1959–2021. Left column DJF, right at JJA **a** 100 hPa, **b** 200 hPa, **c** 500 hPa, **d** 850 hPa, **e** surface

Table 6 Trends (ºC/year) of annual air temperature at T2m, 850, 500, 200, and 100 hPa for the period 1959–2021

	DJF					JJA				
Station	T2m	T850	T500	T200	T100	T2m	T850	T500	T200	T100
Ankara	0.039*	0.030*	0.012*	0.002	−0.021*	0.046*	0.034*	0.025*	0.006	−0.033*
Aswan	0.015*	0.012	0.016*	0.017*	−0.031*	0.022*	0.029*	−0.001	0.012*	−0.027*
Athalassa	0.040*	0.017*	0.009	0.010	−0.022*	0.036*	0.017*	0.012*	0.007	−0.025*
Athens	0.026*	0.017*	0.011	0.003	−0.020*	0.021*	0.019*	0.019*	0.008	−0.026*
Helwan	0.019*	0.012	0.012*	0.014*	−0.024*	0.028*	0.011*	0.011*	0.008*	−0.022*
Heraklion	0.023*	0.011	0.009	0.009	−0.019*	0.008	0.017*	0.015*	0.013*	−0.025*
Izmir	0.023*	0.020*	0.010	0.003	−0.019*	0.034*	0.030*	0.022*	0.008	−0.028*
Matruh	0.010	0.010	0.007	0.012*	−0.018*	0.022*	0.010*	0.012	0.010*	−0.023*
Thessaloniki	0.033*	0.027*	0.013*	−0.004	−0.022*	0.036*	0.028*	0.025*	0.001	−0.030*

The asterisk indicates statistically significant values at 95% confidence level

Table 7 Pearson correlation coefficient of NAO with at T2m, 850, 500, 200, and 100 hPa for the period 1959–2021

	DJF					JJA				
Station	T2m	T850	T500	T200	T100	T2m	T850	T500	T200	T100
Ankara	−0.039	−0.083	−0.055	0.297*	0.069	−0.277*	−0.297*	−0.415*	0.057	0.157*
Aswan	−0.313*	−0.289*	0.180*	0.074	−0.137	−0.233*	−0.227*	0.057	−0.221*	0.075
Athalassa	−0.079	−0.224*	−0.193*	0.443*	0.098	−0.298*	−0.271*	−0.179*	−0.114	0.055
Athens	0.060	−0.083	−0.031	0.188*	0.012	−0.383*	−0.392*	−0.482*	0.020	0.215*
Helwan	−0.312*	−0.345*	−0.171*	0.370*	0.084	−0.252*	−0.223*	−0.046*	−0.188*	0.036
Heraklion	−0.140	−0.274*	−0.167*	0.343*	0.110	−0.252*	−0.360*	−0.345*	−0.062	0.141
Izmir	0.007	−0.051	−0.024	0.227*	0.034	−0.321*	−0.358*	−0.467*	0.048	0.201*
Matruh	−0.367*	−0.398*	−0.263*	0.400*	0.154*	−0.159*	−0.207*	−0.188*	−0.146*	0.051
Thessaloniki	0.165*	0.112	0.089	0.066	−0.062	−0.354*	−0.380*	−0.493*	0.056	0.270*

The asterisk indicates statistically significant values at 95% confidence level

becomes positive over the Red Sea. The correlation becomes positive almost all over the domain at 200 hPa. In contrast to the correlation on 500 hPa, there was a positive correlation at 100 hPa. Our results are supported with the results presented by Hasanean (2004), who found a negative relationship between surface temperature and NAO index in the wintertime over Egypt. In addition, according to Türkeş and Erlat (2009) in Turkey, winter the temperature is low during the positive phase of the NAO index.

Summer

The correlation in summer (JJA) between NAOI and air temperature differs from that in winter as shown in the right column in Fig. 10. It is negative at the surface and 850 hPa, while at 500 hPa, it turns positive over the Red Sea, which is weaker than that in winter. At 200 hPa, the correlation is negative for all domain areas as in the surface, and at 850 hPa, except above lat 30°N, it becomes positive. The correlation at 100 hPa is positive.

Table 7 shows the Pearson correlation coefficient between NAOI and temperature at T2m, 850, 500, 200, and 100 hPa for the period 1959–2021.

Conclusion

The assessment of the ERA-Interim and ERA-5 reanalysis is compared with upper air variables (*Z*, *T*, Td, and RH) at nine stations over the Eastern Mediterranean region with different climatological characteristics during the period 2000–2017 at the surface and four isobaric levels 850, 700, 500, and 200 hPa. In general, both reanalysis datasets have high concordance with temperature and geopotential height with strong correlation and low mean bias and root-mean-square error in all the examined stations. But it has less correlation and high mean bias and root-mean-square error in all stations with RH and Td in the

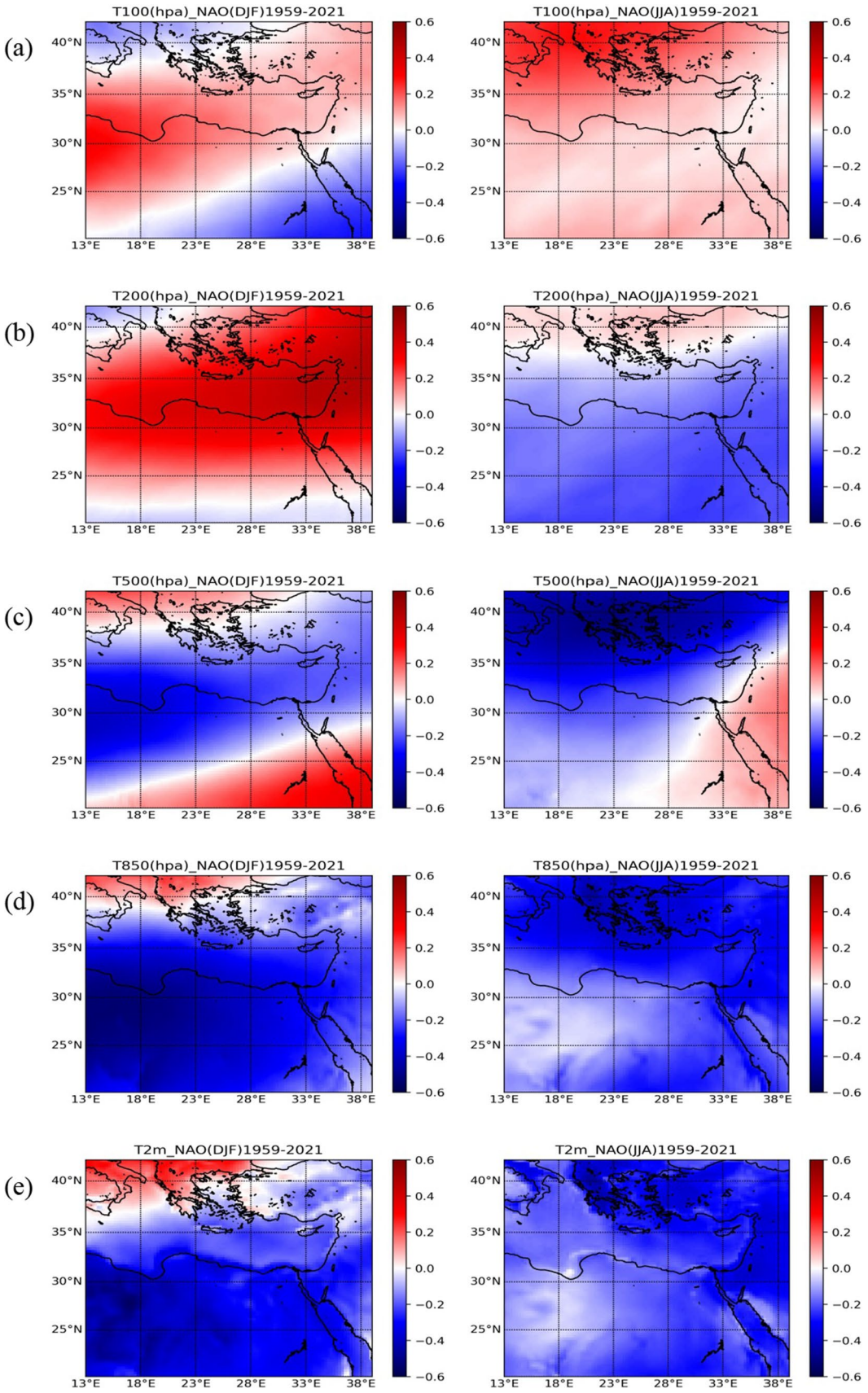

Fig. 10 Surface and upper air temperature correlation with NAOI (1959–2021) left column DJF, right at JJA **a** 100 hPa, **b** 200 hPa, **c** 500 hPa, **d** 850 hPa, **e** surface

upper troposphere. ERA-5 is relatively considered a good representation of upper air variables which is better than ERA-Interim.

In conclusion, ERA-Interim and ERA-5 consist of a valuable source of data that can be used to supplement radiosonde data, and to compensate for the lack of direct observations in the Eastern Mediterranean region, as it was also concluded by (Baatz et al. 2021).

The effects of climate change and greenhouse gases on increasing the surface temperature affect the upper atmosphere, with significant warming in the lower troposphere, and cooling in the upper troposphere and lower stratosphere. Similar results have also been concluded by Philandras et al. (2017) and Elbessa et al. (2021) for the Mediterranean region, and IPCC (2013) as well.

The teleconnection of the NAO index shows a negative correlation with surface and upper air temperature, which turns positive at level 200 hPa in winter and at 100 hPa in summer. The positive (negative) phase of NAO is associated with temperature cooling (warming).

Acknowledgements Authors thank the European Center for Medium-Range Weather Forecasts (ECMWF), National Oceanic and Atmospheric Administration (NOAA), and Wyoming University for providing data to improve the paper.

Funding Open access funding provided by The Science, Technology & Innovation Funding Authority (STDF) in cooperation with The Egyptian Knowledge Bank (EKB). This research received no external funding.

Declarations

Conflict of interest The authors declared that they have no conflict of interest.

References

Al-Hemoud A, Al-Dashti H, Al-Saleh A, Petrov P, Malek M, Elhamoud E, Middleton N (2022) Dust storm 'hot spots' and transport pathways affecting the Arabian Peninsula. J Atmos Sol Terr Phys 238:105932

Baatz R, Hendricks Franssen HJ, Euskirchen E et al (2021) Reanalysis in earth system science: toward terrestrial ecosystem reanalysis. Rev Geophys 59:3. https://doi.org/10.1029/2020RG000715

Bao X, Zhang F (2013) Evaluation of NCEP-CFSR, NCEP-NCAR, ERA-Interim, and ERA-40 reanalysis datasets against independent sounding observations over the Tibetan Plateau. J Clim 26:206–214. https://doi.org/10.1175/JCLI-D-12-00056.1

Dee DP, Uppala SM, Simmons AJ et al (2011) The ERA-Interim reanalysis: configuration and performance of the data assimilation system. Q J R Meteorol Soc 137:553–597. https://doi.org/10.1002/qj.828

Donat MG, Peterson TC, Brunet M et al (2014) Changes in extreme temperature and precipitation in the Arab region: long-term trends and variability related to ENSO and NAO. Int J Climatol 34(3):581–592. https://doi.org/10.1002/joc.3707

Dong Y, Li G, Yuan M, Xie X (2017) Evaluation of five grid datasets against radiosonde data over the eastern and downstream regions of the Tibetan plateau in summer. Atmosphere 8:56. https://doi.org/10.3390/atmos8030056

Elbessa M, Abdelrahman SM, Tonbol K, Shaltout M (2021) Dynamical downscaling of surface air temperature and wind field variabilities over the southeastern levantine basin, mediterranean sea. Climate 9(10):150. https://doi.org/10.3390/cli9100150

Fu G, Charles SP, Timbal B et al (2016) Comparison of NCEP-NCAR and ERA-Interim over Australia. Int J Climatol 36(5):2345–2367. https://doi.org/10.1002/joc.4499

Gleixner S, Demissie T, Diro GT (2020) Did ERA5 improve temperature and precipitation reanalysis over East Africa? Atmosphere 11(9):996. https://doi.org/10.3390/atmos11090996

Guo Y, Zhang S, Yan J et al (2016) A comparison of atmospheric temperature over China between radiosonde observations and multiple reanalysis datasets. J Meteorol Res 30:242–257. https://doi.org/10.1007/s13351-016-5169-0

Hasanean HM (2004) Wintertime surface temperature in Egypt in relation to the associated atmospheric circulation. Int J Climato 24(8):985–999. https://doi.org/10.1002/joc.1043

Hersbach H (2016) The ERA5 atmospheric reanalysis. In: Proceedings of the AGU Fall Meeting Abstracts, San Francisco, CA, USA, 12–16 December 2016; Volume 2016, p NG33D–01

Hurrell JW, Deser C (2009) North atlantic climate variability: the role of the north Atlantic oscillation. J Mar Syst 79(3–4):231–244. https://doi.org/10.1016/j.jmarsys.2008.11.026

IPCC (2013) Summary for policymakers climate change. The Physical Science Basis. Contribution of Working Group I to the Fifth Assessment Report of the Intergovernmental Panel on Climate Change Cambridge University Press IPCC AR5

Johns RH, Doswell CA (1992) Severe local storms forecasting. Wea Forecast 7(4):588–612

Marshall GJ (2002) Trends in Antarctic geopotential height and temperature: a comparison between radiosonde and NCEP-NCAR reanalysis data. J Clim 15:659–674. https://doi.org/10.1175/1520-0442(2002)015%3c0659:TIAGHA%3e2.0.CO;2

Mooney PA, Mulligan FJ, Fealy R (2011) Comparison of ERA-40, ERA-Interim and NCEP/NCAR reanalysis data with observed surface air temperatures over Ireland. Int J Climatol 31(4):545–557. https://doi.org/10.1002/joc.2098

Orlanski I (1975) A Rational subdivision of scales for atmospheric processes. Bull Am Meteorol Soc, 56(5), 527–530. http://www.jstor.org/stable/26216020

Philandras CM, Nastos PT, Kapsomenakis IN, Repapis CC (2015) Climatology of upper air temperature in the Eastern Mediterranean region. Atmos Res 152:29–40. https://doi.org/10.1016/j.atmosres.2013.12.002

Philandras CM, Kapsomenakis J, Nastos PT, et al (2017) Climatology of upper air temperature over the Mediterranean. Trends and Variability. In Perspectives on Atmospheric Sciences, pp 565–576. Springer, Cham. https://doi.org/10.1007/978-3-319-35095-0_81

Shaltout M, El Gindy A, Omstedt A(2013) Recent climate trends and future scenarios in the Egyptian Mediterranean coast based on

six global climate models. Geofiz J 30:19–41, UDC 551.581.1, 551.588.7. https://hrcak.srce.hr/105849

Stickler A, Storz S, Wartenburger R et al (2015) Upper-Air observations from the German atlantic expedition (1925–27) and comparison with the twentieth century and ERA-20C reanalyses. Meteorol Z 24(5):525–544. https://doi.org/10.1127/metz/2015/0683

Tan E (2019) Evaluation of NCEP/NCAR reanalysis Precipitable water data comparing to radiosonde observations for Turkey. Cumhur Sci J 40(2):527–535

Taylor KE (2001) Summarizing multiple aspects of model performance in a single diagram. J Geophys Res Atmos 106(D7):7183–7192. https://doi.org/10.1029/2000JD900719

Tonbol KM, El-Geziry TM, Elbessa M (2018) Evaluation of changes and trends in air temperature within the Southern Levantine basin. Weather 73(2):60–66. https://doi.org/10.1002/wea.3186

Türkeş M, Erlat E (2009) Winter mean temperature variability in Turkey associated with the North Atlantic oscillation. Meteorol Atmos Phys 105:211–255. https://doi.org/10.1007/s00703-009-0046-3

Woyciechowska J, Bąkowski R (2006) Comparison of values of the chosen meteorological fields measured at the aerological stations and the values taken from NCEP/NCAR Reanalysis. Időjárás 110(2):183–189